• Clinical Research •

Diagnostic evaluation of optical coherence tomography parameters in normal, preperimetric and perimetric glaucoma patients

Aimy Mastura Zurairah Yusof[1], *Othmaliza Othman*[2], *Seng Fai Tang*[2], *Mohd Rohaizat Hassan*[3], *Norshamsiah Md Din*[2]

[1]Department of Ophthalmology, Tuanku Mizan Armed Forces Hospital, Kuala Lumpur 53300, Malaysia
[2]Department of Ophthalmology, UKM Medical Center, Jalan Yaacob Latif, Cheras 56000, Kuala Lumpur, Malaysia
[3]Department of Community Health, UKM Medical Center, Jalan Yaacob Latif, Cheras 56000, Kuala Lumpur, Malaysia
Correspondence to: Norshamsiah Md Din. Department of Ophthalmology, UKM Medical Center, Jalan Yaacob Latif, Cheras 56000, Kuala Lumpur, Malaysia. shamsiahdr@hotmail.com
Received: 2020-11-20 Accepted: 2022-05-14

Abstract

• **AIM:** To compare the diagnostic ability of glaucoma parameters measured by the optical coherence tomography (OCT) in normal, preperimetric glaucoma (PPG) and perimetric glaucoma (PG) patients.

• **METHODS:** This cross-sectional observational study includes 127 eyes of 127 subjects. Patients were divided into PPG (51 eyes), PG (46 eyes), and normal controls (30 eyes) based on clinical optic disc assessment and Humphrey visual field changes. The Heidelberg Spectralis OCT machine using Glaucoma Module Premium Edition software was used to measure the retinal nerve fiber layer (RNFL) and Bruch's membrane opening-minimum rim width (BMO-MRW) to assess the optic nerve head and ganglion cell layer (GCL) thickness in the macula.

• **RESULTS:** RNFL, MRW, and GCL thickness were all significantly thinner in PG compared to PPG and the normal group. The BMO-MRW parameters showed better specificity (>70%) at 90% specificity compared to both RNFL and GCL parameters to discriminate normal, PPG, and PG patients. All BMO-MRW parameters showed higher area under curves (AUC) compared to RNFL and GCL parameters with the highest AUC observed in the superotemporal sector of the BMO-MRW (AUC=0.819 and and 0.897 between normal and PPG and PG groups respectively).

• **CONCLUSION:** While the BMO-MRW best discriminates PPG and PG against normal eyes, GCL parameters poorly differentiate the three groups.

• **KEYWORDS:** glaucoma; preperimetric; ganglion cell layer; Bruch's membrane opening; minimum rim width; retinal nerve fibre layer

DOI:10.18240/ijo.2022.11.08

Citation: Yusof AMZ, Othman O, Tang SF, Hassan MR, Din NM. Diagnostic evaluation of optical coherence tomography parameters in normal, preperimetric and perimetric glaucoma patients. *Int J Ophthalmol* 2022;15(11):1782-1790

INTRODUCTION

Glaucoma is the second leading cause of vision loss in the world[1]. It is a group of diseases characterized by structural damage to the optic nerve head (ONH) and characteristic glaucomatous field defects[2]. It mostly affects the superior and inferior poles of the optic disc resulting in an increase in the vertical cup:disc ratio (VCDR), a simple and robust index to assess neuroretinal loss in glaucoma[2].

Glaucoma can be classified according to the mechanism of damage into primary open angle glaucoma (POAG), primary angle-closure glaucoma (PACG), secondary glaucoma, and glaucoma suspect (GS). Primary angle-closure can be further classified into primary angle-closure suspect (PACS), primary angle-closure (PAC), and PACG[2].

Glaucoma is staged based on the degree of the visual field (VF) defect into early, moderate and severe defects following the Hodapp, Parrish, and Anderson's Classification[3], or the Brusini Glaucoma Staging System 2 (GSS2)[4]. The GSS2 classification uses humphrey visual field (HVF) measured parameters like mean deviation (MD), corrected pattern standard deviation (CPSD), and corrected loss variance (CLV). In circumstances where CPSD and CLV are not available, pattern standard deviation (PSD) or loss variance (LV) can be used.

Bruch's membrane opening-minimum rim width (BMO-MRW) is an optical coherence tomography (OCT) measurement that provides an anatomically and geometrically accurate parameter to measure the neuroretinal rim width. It measures the BMO which is the accurate outer border of the neuroretinal rim

(NRR), representing the maximum aperture from which the retinal ganglion cell (RGC) axons exit the globe[5]. The BMO-MRW is measured in 24-star sectors across the ONH and provides an accurate measurement of the actual rim width.

The retinal nerve fibre layer (RNFL) thickness was shown to have a variable ability to discriminate glaucomatous from normal eyes[6-7]. The peripapillary RNFL thickness was previously used to monitor the progression of RNFL thinning in glaucoma patients on the basis that anatomical changes of the ONH precedes glaucomatous field changes[8].

The ganglion cell complex (GCC) thickness is another widely studied parameter for monitoring glaucoma progression. However, the GCC includes not just the nerve fibre layer (NFL) and ganglion cell layer (GCL), but also the inner plexiform layer (IPL)[9]. With better technology, the OCT is now able to discern and measure the GCL thickness alone, the most affected layer of the retina in patients with glaucoma[10-13]. Because of variable reports on these three major parameters used for glaucoma diagnosis, we aim to evaluate which of the three parameters has the best diagnostic ability in three groups of patients: normal, preperimetric glaucoma (PPG), and perimetric glaucoma (PG), and compare the sensitivity and specificity in discriminating the three groups of patients.

SUBJECTS AND METHODS

Ethical Approval Ethical approval was obtained from the Universiti Kebangsaan Malaysia Research and Ethics Committee (Ethical approval code: FF-2017-169). This study adhered to the tenets of the Declaration of Helsinki and the Malaysian Guidelines for Good Clinical Practice (GCP). A signed written informed consent was obtained from all patients prior to enrolment.

This was a cross-sectional observational study where participants were consecutively recruited in a tertiary referral center from April 2017 to April 2018. The eligibility of the participants was determined by a complete ophthalmic examination including slit-lamp biomicroscopy, intraocular pressure measurement using the Goldman applanation tonometer, dilated fundus examination, retina tomography scan, and VF test. Only the right eye was taken from each participant for the purpose of standardisation. In the perimetric group, the better eye was chosen to be able to evaluate the ability of the OCT parameters to discern between PPG and less severe PG.

The PPG patients were those with glaucomatous features on the optic disc such as VCDR>0.7 and/or notching or rim thinning, but with a normal HVF test[14]. OCT changes were not required to define PPG[14-15]. The PG patients were those with glaucomatous disc changes and VF loss detected by the HVF. An experienced glaucoma specialist (Din Nin) made the diagnosis of PPG and PG. The PG patients were further divided into mild, moderate, and severe glaucoma based on Brusini's GSS2 classification system[4]. The normal group has neither of both.

The inclusion criteria include participants aged between 18-70 years old and diagnosed with PPG or PG. The participants in the normal group must not have the criteria of the PPG and PG group. Exclusion criteria include any media opacity preventing good signal quality of the OCT, pre-existing retinal diseases such as proliferative diabetic retinopathy or maculopathy; or lasered-retina. Optic neuropathies other than glaucoma such as compressive or ischaemic optic neuropathy were also excluded. Other unusual or abnormal optic disc appearance not attributed to glaucoma, like optic disc pit, tilted myopic disc, and optic atrophy, was excluded. Based on a power analysis, the number of sample size collected gave power of study of at least 70%.

Humphrey Visual Field The VF was mapped with the HVF Analyzer (Carl Zeiss Meditec Dublin, CA, USA) using the Swedish Interactive Threshold Algorithm (SITA) standard 24-2. Patients in the PG group was further classified into mild, moderate, and severe glaucoma using the Brusini classification based on the MD and PSD level[4]. Only VF with reliable indices was included, which are fixation loss of less than 20% and false-negative and positive errors of less than 33%.

Optical Coherence Tomography Retinal tomography was done using the Heidelberg Spectralis OCT Plus machine (Spectralis HRA+OCT; Heidelberg Engineering) with the Glaucoma Module Premium Edition (GMPE) software version 6.0f after pharmacologic dilatation. The OCT scans were performed by three experienced technicians who have performed OCT scans for at least 5y. OCT scans with signal strengths of less than 20 dB were deemed to have poor signal strength as recommended by the manufacturer, and therefore excluded. Each eye had 3 images taken, one each for the RNFL circular scan, the BMO-MRW, and the GCL scans of the macula. While all OCT printouts were checked for faulty automated measurements, the automated segmentation of retinal layers was not manually controlled.

The RNFL thickness (μm) was measured in 6 sectors (superotemporal, superonasal, nasal, inferonasal, inferotemporal, and temporal). Using the anatomical position system (APS) in the GMPE software, the fovea and the center of BMO were identified as the 2 fixed anatomical location. The APS uses the participants' anatomic landmark to automatically position and aligns the individual fovea-BMO center axis. The BMO-MRW measurement was obtained using 24 star-pattern scans to measure the size of the BMO area (mm²) and MRW thickness (μm) in 6 sectors (superotemporal, superonasal, nasal, inferonasal, inferotemporal and temporal). The MRW thickness was obtained by measuring the nearest distance from the edge of BMO to the internal limiting membrane (ILM).

The GCL thickness was obtained using horizontal scans of the posterior pole with an elliptical grid of 1, 3, and 6 mm superimposed on the macular region. The machine will automatically segment the retina layer-by-layer to obtain the GCL thickness separately. We used a larger grid to get a higher diagnostic ability[16]. GCL volume (mm^3) and 4 sectors (superior, nasal, inferior, and temporal) of GCL thickness in the 3 to 6 mm grid diameters were taken as they were shown to best discriminate between early glaucoma and normal patients[17]. Macula printouts were checked for the presence of other confounders like epiretinal gliosis, macula edema or any other macular pathology, and were excluded.

Data Analysis Statistical analyses were performed using SPSS software (version 22.0; SPSS Inc., Chicago, IL, USA). The normality of the data was analyzed using a histogram with normality plots, skewness & kurtosis, and Kolmogorov-Smirnov statistic. One-way analysis of variants (ANOVA) tests were used to analyze the RNFL, MRW, and GCL thickness among the normal, PPG, and PG groups. Receiver operating characteristic (ROC) curve analysis was conducted to evaluate and compare the diagnostic ability of individual OCT parameters. The area under curves (AUC) was calculated for the RNFL, BMO-MRW, and GCL thickness. As we are comparing the diagnostic ability of these three parameters to differentiate between normal, PPG, and PG eyes, the gold standard was the glaucoma status of the participants (PG, PPG, and normal group) as defined by glaucomatous optic disc assessment and the patients' VF.

RESULTS

A total of 127 participants were enrolled in this study, with 30 normal subjects, 51 PPG, and 46 PG patients (Table 1). Chinese ethnicity made up the most number of participants. There was no significant difference in age and gender distribution between the three groups.

Among the 46 PG patients, 19 (41.3%) were classified as mild, 16 (34.8%) moderate, and 11 (23.9%) severe glaucoma. Twenty-seven (58.7%) patients were diagnosed with POAG, 15 (32.6%) were diagnosed with NTG, and 4 (8.7%) patients had PACG.

Retinal Nerve Fibre Layer Measurement The mean RNFL thickness of all sectors is highest in the normal group followed by the PPG and PG group. A one-way between-subjects ANOVA was conducted to compare the RNFL thickness among the normal, PPG, and PG groups (Table 2). There was a significant difference in the RNFL thickness of all sectors (P<0.05). Post Hoc test using least significant difference (LSD) formula showed there was a significant difference in RNFL thickness in the superonasal, and inferonasal sector between the three groups. The nasal RNFL thickness was only significantly different between normal and both PPG and PG and not between the PPG and PG groups. In the inferotemporal and temporal sector, the difference lies only between PG and PPG groups, and between normal and PG groups respectively.

Bruch Membrane Opening and Minimum-Rim-Width Measurement The mean size of the BMO area was smallest in the normal group followed by PPG and PG group (Table 2). However, the mean size of the BMO area was also smallest in the moderate compared to mild and severe glaucoma group of the PG patients, and this difference was statistically significant (P<0.05). The BMO-MRW values were also thinner in moderate compared to mild and severe groups, possibly because of the small number of eyes in the severe group. Post Hoc test using LSD formula showed that the BMO area was significantly different between normal and both PPG and PG groups. The mean MRW thickness is lowest in the PG group followed by PPG and normal participants and this was also statistically significant, P<0.05. Posthoc comparison using the LSD test revealed that a significant difference in MRW thickness was seen in all sectors between the three groups.

Ganglion Cell Layer Thickness Measurement Macular GCL thickness was measured using the largest elliptical grid, each composed of three rings, an inner, middle, and outer ring of 1, 3, and 6 mm. We measured the GCL thickness of the outer 3-6 mm grid which shows early changes seen in the initial stages of glaucomatous damage. We found a significant difference in the GCL average volume, outer superior GCL, outer nasal GCL, outer inferior GCL, and outer temporal GCL thickness in the normal, PG, and PPG groups (P<0.05). Posthoc comparison using LSD test showed that the GCL average volume, outer superior GCL, outer nasal GCL, outer inferior GCL, and outer temporal GCL thickness significantly differ between PG and both normal and PPG group. All GCL parameters, however, showed no significant difference between PPG and normal groups.

Diagnostic Ability of RNFL, BMO-MRW, and GCL Thickness Scans AUC values were calculated to assess and compare the diagnostic ability of the three parameters. All BMO-MRW parameters showed higher AUC compared to RNFL and GCL parameters, indicating a higher diagnostic accuracy of MRW parameters when comparing between normal and PG (Figure 1) and PPG groups (Figure 2). The highest AUC was seen in the superotemporal quadrant of the BMO-MRW (AUC=0.897 and 0.819 between normal and PG and PPG eyes respectively). While the AUC for RNFL has a fair score in its ability to diagnose glaucoma, GCL parameters performed poorly in its ability to differentiate glaucoma from the normal population.

Among patients in the PG group, the sensitivity was highest at the inferotemporal sector of the BMO-MRW (sensitivity of 75% when specificity was fixed at 90%, and 68.2% when specificity was fixed at 95%) compared to all other parameters

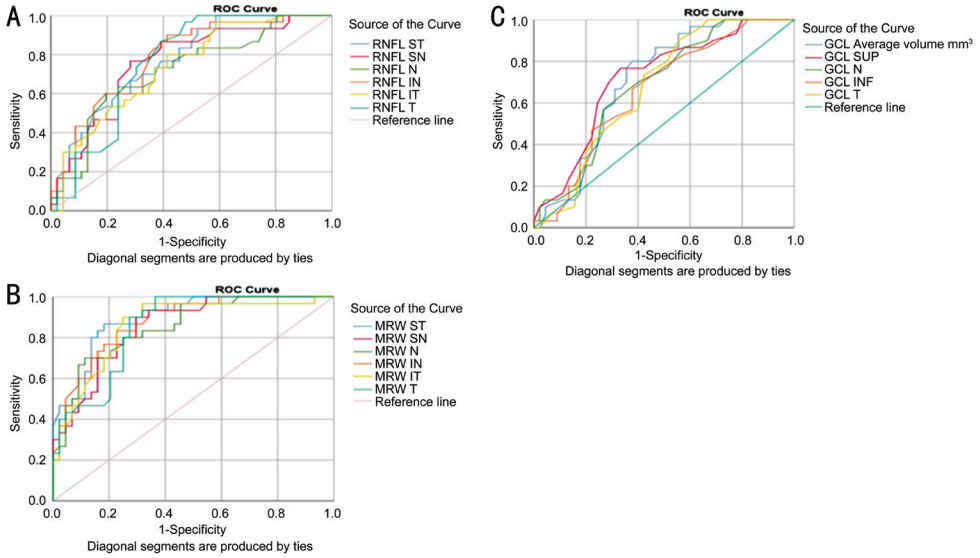

Figure 1 The area under the receiver operator curve (AUC) of different OCT parameters between the PG group and the normal population A: AUC for RNFL thickness; B: AUC for MRW thickness; C: AUC for GCL thickness. RNFL: Retinal nerve fiber layer; MRW: Minimum rim width; GCL: Ganglion cell layer.

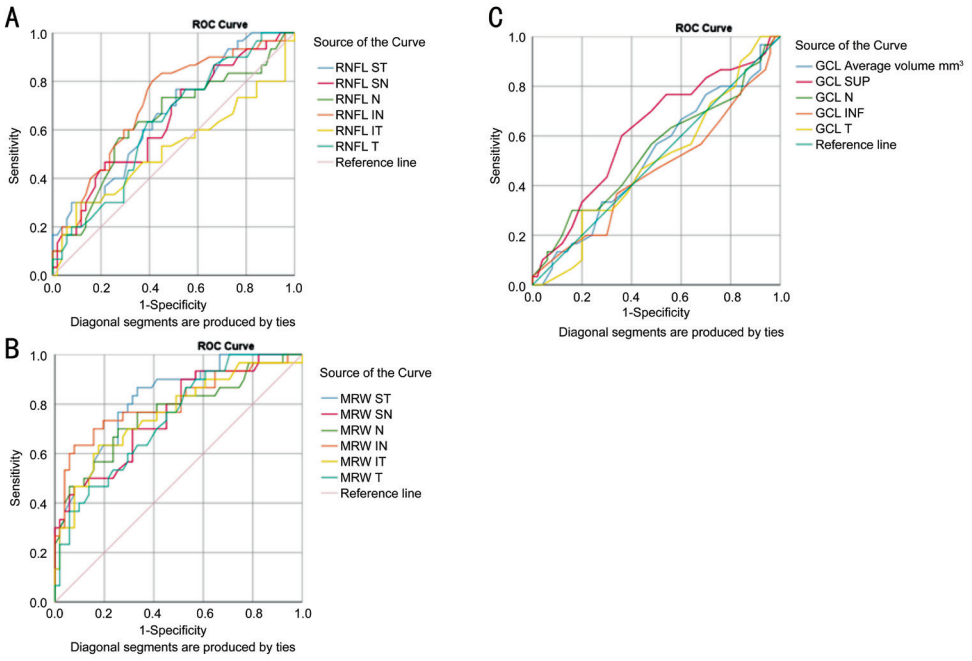

Figure 2 The area under the receiver operator curve (AUC) between the PPG group and the normal population A: AUC for RNFL thickness; B: AUC for MRW thickness; C: AUC for GCL thickness. RNFL: Retinal nerve fiber layer; MRW: Minimum rim width; GCL: Ganglion cell layer.

Table 1 Demographics and ocular characteristics of subjects

Parameters	Normal, *n*=30	PPG, *n*=51	PG, *n*=46	Total, *n*=127	*P*
Age, median (IQR)	64.0 (57.5-70)	65.0 (61-70)	69.0 (66-70)		0.22[a]
Gender, *n* (%)					0.38[b]
Male	10 (33.3)	19 (37.3)	22 (47.8)	51 (40.2)	
Female	20 (66.7)	32 (62.7)	24 (52.2)	76 (59.8)	
Race, *n* (%)					0.41[b]
Malay	14 (46.7)	20 (39.2)	14 (30.4)	48 (37.8)	
Chinese	15 (50.0)	24 (47.1)	27 (58.7)	66 (52.0)	
Indian	1 (3.3)	7 (13.7)	5 (10.9)	13 (10.2)	
IOP (mm Hg), median (IQR)	16.0 (14.0-16.25)	14.0 (12.0-16.0)	14.0 (12.0-14.25)		0.02[a]

IOP: Intraocular pressure; IQR: Interquartile range; PPG: Prepermetric glaucoma; PG: Perimetric glaucoma; [a]Kruskal wallis test; [b]Chi-square test.

Table 2 Mean thickness of different optical coherence tomography parameters μm, mean±SD

Parameters	Normal	PPG	PG					*P* value from post hoc analysis[b]		
			Overall	Mild	Moderate	Severe	*P*[a]	Normal *vs* PPG	Normal *vs* PG	PPG *vs* PG
RNFL global	103.93±10.46	94.41±10.92	81.26±20.31	91.16±17.91	72.88±15.34	76.36±24.51	<0.001	0.006	<0.001	<0.001
RNFL ST	143.5±20.51	128.76±24.03	114.41±31.67	127.89±27.09	106.63±25.16	102.45±40.55	<0.001	0.17	<0.001	0.008
RNFL SN	113.8±25.55	100.67±24.19	89.15±28.12	98.32±28.0	77.31±20.72	90.55±33.41	<0.001	0.03	<0.001	0.031
RNFL IN	116.63±22.39	101.51±21.73	86.83±29.12	98.05±23.93	71.31±21.79	90.0±37.89	<0.001	0.01	<0.001	0.004
RNFL IT	139.53±27.62	138.69±20.43	109.83±39.23	127.74±31.10	101.0±30.73	91.73±51.71	<0.001	0.9	<0.001	<0.001
RNFL N	74.57±19.58	64.88±17.49	58.93±19.53	68.58±16.56	50.81±16.63	54.09±22.35	0.002	0.03	0.001	0.121
RNFL T	80.57±10.8	74.82±12.09	66.26±18.16	70.05±19.75	63.06±15.67	64.36±19.13	<0.001	0.84	<0.001	0.004
BMO area (mm²)	1.98±0.36	2.37±0.46	2.45±0.53	2.52±0.57	2.30±0.45	2.54±0.57	<0.001	0.001	<0.001	0.405
MRW global	287.80±58.71	245.39±28.772	201.86±55.51	223.16±52.65	179.60±43.71	194.80±66.11	<0.001	<0.001	<0.001	<0.001
MRW ST	301.1±45.87	241.02±47.09	197.57±66.71	216.58±58.99	181.80±57.60	185.10±88.26	<0.001	<0.001	<0.001	<0.001
MRW SN	340.53±63.17	278.53±52.02	237.27±72.18	265.32±66.65	217.47±58.82	213.70±87.73	<0.001	<0.001	<0.001	0.002
MRW N	318.33±62.43	262.75±45.62	220.91±68.30	253.11±60.91	187.73±58.90	209.50±72.82	<0.001	<0.001	<0.001	0.001
MRW IN	359.73±67.35	291.90±43.14	242.73±75.31	257.47±79.18	220.80±56.40	247.60±91.23	<0.001	<0.001	<0.001	<0.001
MRW IT	305.77±56.59	264.31±41.57	211.48±70.10	242.68±56.52	188.0±55.19	187.40±93.43	<0.001	0.002	<0.001	<0.001
MRW T	203.77±35.18	172.04±31.88	145.0±41.10	156.79±36.71	126.60±35.87	150.20±49.87	<0.001	<0.001	<0.001	<0.001
GCL OS	33.70±4.36	31.88±4.61	29.47±5.72	30.39±6.24	28.38±5.02	29.55±6.06	0.002	1.117	<0.001	0.02
GCL ON	38.0±4.21	37.28±3.78	34.02±6.38	35.94±5.15	31.69±6.80	34.27±7.03	0.001	0.531	0.001	0.002
GCL OI	29.70±4.13	30.16±3.64	26.91±5.63	28.83±4.54	25.81±5.62	25.36±6.76	0.002	0.663	0.011	0.001
GCL OT	32.07±3.78	32.08±5.03	28.56±6.20	31.39±4.85	27.19±5.34	25.91±7.83	0.002	0.991	0.005	0.001

PPG: Preperimetric glaucoma; PG: Perimetric glaucoma; RNFL: Retinal nerve fibre layer; BMO: Bruch's membrane opening; MRW: Minimum-rim-width; GCL: Ganglion cell layer; ST: Superotemporal; SN: Superonasal; IN: Inferonasal; IT: Inferotemporal; OS: Outer superior; OI: Outer inferior; OT: Outer temporal; ON: Outer nasal; [a]Analysis of variance; [b]Post hoc analysis using least significant difference formula.

Table 3 Comparison of sensitivity, specificity, and AUC between RNFL, MRW, and GCL parameters in the PG and normal group

Parameters	AUC	95%CI	Sensitivity	
			Specificity fixed at 90%	Specificity fixed at 95%
RNFL G	0.854	0.770-0.938	60.9%	58.7%
RNFL ST	0.771	0.668-0.875	47.8%	41.3%
RNFL SN	0.760	0.650-0.870	43.5%	41.3%
RNFL N	0.717	0.599-0.836	28.3%	23.9%
RNFL IN	0.782	0.678-0.885	58.7%	50.0%
RNFL IT	0.737	0.626-0.848	43.5%	41.3%
RNFL T	0.762	0.655-0.868	54.3%	52.2%
BMO-MRW G	0.869	0.782-0.955	70.5%	65.9%
BMO-MRW ST	0.897	0.828-0.965	70.5%	68.2%
BMO-MRW SN	0.855	0.772-0.938	70.5%	65.9%
BMO-MRW N	0.853	0.768-0.939	56.8%	54.5%
BMO-MRW IN	0.877	0.801-0.953	65.9%	63.6%
BMO-MRW IT	0.860	0.772-0.948	75.0%	68.2%
BMO-MRW T	0.855	0.771-0.938	72.7%	68.2%
GCL SUP	0.717	0.600-0.835	31.1%	22.2%
GCL N	0.685	0.566-0.804	42.2%	31.1%
GCL INF	0.660	0.537-0.783	33.3%	24.4%
GCL T	0.676	0.557-0.796	44.4%	40.0%

AUC: Area under the receiver operating curve; RNFL: Retinal nerve fiber layer; BMO-MRW: Bruch's membrane opening-minimum rim width; GCL: Ganglion cell layer; CI: Confidence interval; G: Global; SUP: Superior; INF: Inferior; N: Nasal; T: Temporal; ST: Superotemporal; SN: Superonasal; IN: Inferonasal; IT: Inferotemporal.

(Table 3). The BMO-MRW parameters also showed better sensitivity when specificity is fixed at 90% and 95% as compared to the RNFL and GCL parameters, signifying a higher diagnostic accuracy of BMO-MRW parameters compared to RNFL and GCL parameters in distinguishing glaucomatous from normal eyes (Table 3).

Table 4 Comparison of sensitivity, specificity, and AUROC between RNFL, MRW, and GCL parameters in the PPG and normal group

Parameters	AUC	95%CI	Sensitivity	
			Specificity fixed at 90%	Specificity fixed at 95%
RNFL G	0.727	0.611-0.843	23.5%	23.5%
RNFL ST	0.661	0.541-0.782	29.4%	27.5%
RNFL SN	0.637	0.512-0.762	23.5%	19.6%
RNFL N	0.636	0.506-0.765	13.7%	9.8%
RNFL IN	0.710	0.594-0.826	35.3%	25.5%
RNFL IT	0.521	0.380-0.661	3.9%	3.9%
RNFL T	0.626	0.503-0.749	27.5%	15.7%
BMO-MRW G	0.795	0.677-0.913	33.3%	13.7%
BMO-MRW ST	0.819	0.727-0.911	58.8%	41.2%
BMO-MRW SN	0.758	0.650-0.867	49.0%	43.1%
BMO-MRW N	0.763	0.650-0.876	23.5%	21.6%
BMO-MRW IN	0.805	0.698-0.912	35.3%	31.4%
BMO-MRW IT	0.760	0.649-0.872	39.2%	25.5%
BMO-MRW T	0.740	0.632-0.848	43.1%	39.2%
GCL SUP	0.618	0.490-0.746	10.0%	6.0%
GCL NASAL	0.537	0.402-0.672	8.0%	6.0%
GCL INF	0.461	0.326-0.595	6.0%	4.0%
GCL TEMP	0.493	0.364-0.623	16.0%	12.0%

AUC: Area under the receiver operating curve; RNFL: Retinal nerve fiber layer; BMO-MRW: Basement membrane opening-Minimum rim width; GCL: Ganglion cell layer; CI: Confidence interval; G: Global; SUP: Superior; INF: Inferior; N: Nasal; TEMP/T: Temporal; ST: Superotemporal; SN: Superonasal; IN: Inferonasal; IT: Inferotemporal.

The sensitivities of all parameters in differentiating normal from PPG groups were lower when specificity was fixed at 95% and 90%. Again, the highest sensitivity was observed in the superotemporal sector of the BMO-MRW (58.8% and 41.2% sensitivity at 90% and 95% specificity respectively; Table 4). All MRW parameters showed a fair level of AUC compared to RNFL and GCL parameters, which emphasize a fairly better diagnostic accuracy (Figure 2). The RNFL AUC scores fairly in differentiating PPG from the normal population. The GCL parameters however had the lowest AUC values.

DISCUSSION

The objectives of this study were mainly to evaluate the diagnostic ability of the three major glaucoma parameters using the Heidelberg Spectralis OCT Plus machine with GMPE software version 6.0 to differentiate between the normal population, PPG, and PG group of eyes. Previous studies either compared only healthy individuals and those with glaucoma or between different stages of glaucoma severity. We included moderate and severe glaucoma in our study to reflect the real-world situation when dealing with glaucoma cases in clinical practice.

Agreeing with previous studies that found BMO-MRW to have higher diagnostic accuracy and superiority[7,18-19], we found a significant difference in all sectors of BMO-MRW thickness between the three groups. The RNFL thickness also showed significant difference except for a few sectors. The BMO-MRW parameters have the highest diagnostic ability to discriminate PPG and PG against normal eyes, compared to RNFL and GCL parameters. This is especially so in the supertemporal sector of MRW with the highest AUC indicating its highest diagnostic ability. This is probably seen because, as opposed to RNFL and GCL, the BMO-MRW thickness is made up of ganglion cell axons in its entirety, the very type of cells affected by glaucomatous damage.

Chauhan *et al*[7] found that the BMO-MRW had a better discriminating ability compared to RNLF thickness. Globally, BMO-MRW yielded better diagnostic performance than the other parameters. At 95% specificity, the sensitivity of RNFL thickness, BMO-HRW, and BMO-MRW was 70%, 51%, and 81%, respectively, which is higher than ours (60.9% and 70.5% sensitivity for global RNFL and BMO-MRW respectively) probably because of the difference in patient selection and recruitment. Other studies have found comparable AUCs between RNFL and BMO-MRW[20]. We also found that the global BMO-MRW and RNFL thickness were both comparable although the BMO-MRW was a notch higher than RNFL. As the measurement of the BMO-MRW is dependent on the size of the ONH, Kromer and Spitzer[21] found that the discriminating ability of BMO-MRW measurement still showed superiority over other parameters after correcting for the ONH size.

However, there were situations when BMO-MRW was non-superior to the RNFL. When the linear discriminant function was applied, Bambo *et al*[22] found that BMO-MRW were comparable to the RNFL parameter with no statistical difference between both AUCs when discriminating between normal and mild POAG patients. BMO-MRW were also non-superior to RNFL with similar AUCs between the two parameters (P>0.05) in myopic eyes with visible myopic changes such as tilted disc as reported by Malik *et al*[23].

Chauhan *et al*[24] also recently looked at the effect of aging in individuals aged between 20 to 90 years old in a cross-sectional study and examined the GCL, RNFL, and BMO-MRW. They found a significant decline in all parameters and a stronger relationship between GCL and aging compared with the other two parameters. They postulated that because of this relationship, the GCL might have a better discriminating ability than the other two parameters.

Our result showed that the RNFL, MRW, and GCL thickness was significantly lower in the PG group compared to the PPG and normal groups. This reduction in thickness was especially seen in BMO-MRW and RNFL parameters as compared to GCL layer thickness. We also found that the BMO area was the smallest in the normal group compared to the other two groups. One might wonder whether glaucoma not only causes thinning of the optic nerve rim but also enlargement of the BMO area where RGC axons exit the globe. However, the sample size is too small to make any postulations on this, and the difference could perhaps result from heterogeneous recruitment.

Previous macular topographic studies showed that the GCL is thinner at the temporal compared to the nasal region and inferior compared to the superior region in the normal human retina[25]. We found similar findings with thinner temporal than nasal; and thinner inferior than superior GCL thickness, not just in normal individuals, but also in the PPG and PG group of patients. However, in our study, inferior GCL is not one of the main predictors for developing glaucoma although generally it has been shown to be affected first apart from temporal GCL in patients with glaucoma[26].

GCL parameters however perform poorly in differentiating glaucomatous from non-glaucomatous eyes and between normal and PPG in our cohort of patients. This is in contrast with previous studies which reported that GCL parameters have a better diagnostic ability compared to RNFL parameters[27]. Nevertheless, there were an abundant body of evidence reporting otherwise, agreeing with our results.

While GCL was found to be superior than RNFL in other neuro-ophthalmic diseases[28-29], the same superiority was not seen in glaucoma as results from a Meta-analysis by Oddone *et al*[30], observed that the sensitivity of most parameters for RNFL and macular GCC was between 0.65 and 0.75, making each of these unsatisfactory as a single parameter to be used in a clinical setting. Their Meta-analysis looked at different OCT instruments and differing GCC parameters. They found that the RNFL parameters are still preferred than macular measurements for diagnosis of manifest glaucoma, though differences may be small. However, they also concluded that, because of high heterogeneity, direct comparative or randomized studies of OCT devices or OCT parameters and diagnostic strategies were paramount. Even across different OCT machines, Kansal *et al*[31] in their Meta-analysis of 5 OCT devices found similar diagnostic accuracy between RNFL and segmented macular regions [ganglion cell layer-inner plexiform layer (GCL-IPL), GCC], and higher than total macular thickness. The AUCs were more diagnostically favorable in patients with more severe glaucoma.

We have shown that even though we included various types of glaucoma with varying degrees of severity, RNFL still fares better than the GCL parameter in our cohort of patients, agreeing with other authors who found non-superiority between GCL and papillary RNFL to diagnose PPG[16]. Chauhan *et al*[24] extrapolated from their cross-sectional study involving individuals aged between 20-90 years old that GCL thickness can be better suited to measure the progression of structural glaucomatous loss. They came to this conclusion after they found a significant decline in GCL thickness, MRW, and peripapillary RNFL thickness with age and a stronger relationship between aging and GCL thickness than with the rim or peripapillary RNFL thickness.

Even when different layers of macula measurements were evaluated, the discriminating ability of macula layers was still non-superior to RNFL thickness. Deshpande *et al*[32] evaluated the diagnostic ability of the macular GCL-IPL for detection of PPG and PG and compared it with peripapillary RNFL. They found the RNFL had a better diagnostic ability when compared to GCL-IPL for detecting PPG and PG, although the difference was small and perhaps clinically irrelevant. Na *et al*[33] evaluated the diagnostic abilities of the macula layers compared to the peripapillary RNFL and ONH measurements in the detection of PPG. They found that the global volume loss and superior GCC thickness showed the largest AUC which was 0.84 in each parameter, comparable to the global peripapillary RNFL (0.89) and horizontal cup:disc ratio AUC values (0.85) in their study. When using the GCL layer in combination with an IPL (GCL-IPL thickness) on high definition OCT, Kaushik *et al*[34] found the diagnostic ability of GCL-IPL in PPG was less than ONH and RNFL parameter, and that GCL-IPL do not outperform RNFL measurements in the diagnosis of PPG.

There are different variations in the number of retinal GCC in human eyes and there is a direct relationship between GCC and

GCL thickness. There are approximately 1 million RGCs in the human retina and about 50% of them are concentrated at 4.5-5 mm of the fovea center[25,35]. The GCL thickness measurement at 3 to 6 mm macular grid was taken as it is the best sector to discriminate between normal individuals and PG patients[17]. We found that the GCL thickness significantly differs in the PG group compared to PPG and normal population. However, we found no significant difference in GCL thickness between the normal and PPG group. Although Chauhan *et al*[24] found stronger associations between aging and GCL loss than other parameters, the machanism of RGC loss in glaucoma is not related to aging alone, and therefore GCL loss is not seen more than the other parameters in glaucoma.

In clinical practice, MRW may help to complement the diagnosis of glaucoma in patients who have borderline HVF analysis especially those who fall in the PPG group. This applies to all types of glaucoma, either POAG, PACG, or NTG. The use of the GCL parameter to diagnose early glaucoma must be used with caution especially in non-POAG patients.

We acknowledge the small number of subjects in each subcategory of the PG group (mild, moderate, and severe glaucoma), and is probably inadequate to give meaningful analysis among them. Additionally, other confounding factors to OCT measurements such as refractive errors should also be included in the study.

We conclude that the MRW scan gives a better predictive value in diagnosing glaucoma compared to RNFL and GCL thickness. Those in the PPG group with thinner BMO-MRW may be followed-up more frequently for early detection of conversion into glaucoma in the future.

ACKNOWLEDGEMENTS

The authors would like to thank Nurul Hakimah Samsudin, Syahrul Bariah Surturi, and Nurul Azlina Omar, the assistant medical science officers in UKMMC for helping with the acquisition of the OCT images.

Authors' contributions: All authors contributed to the study concept and design. Material preparation, data collection, and analysis were performed by Yusof AMZ and Hassan MR. The first draft of the manuscript was written by Yusof AMZ and all authors commented on previous versions of the manuscript. All authors read and approved the final manuscript.

Foundations: Supported by Norshamsiah Md Din receives funding from the UKMMC Fundamental Research Grant (No. FF-2017-169); Yusof AMZ receives a Masters scholarship funded by the Government of Malaysia.

Conflicts of Interest: Yusof AMZ, None; **Othman O,** None; **Tang SF,** None; **Hassan MR,** None; **Din NM,** None.

REFERENCES

1 Kulkarni U. Early detection of primary open angle glaucoma: is it happening? *J Clin Diagn Res* 2012;6(4):667-670.

2 Foster PJ, Buhrmann R, Quigley HA, Johnson GJ. The definition and classification of glaucoma in prevalence surveys. *Br J Ophthalmol* 2002;86(2):238-242.

3 Brusini P, Johnson CA. Staging functional damage in glaucoma: review of different classification methods. *Surv Ophthalmol* 2007; 52(2):156-179.

4 Brusini P, Filacorda S. Enhanced Glaucoma Staging System (GSS 2) for classifying functional damage in glaucoma. *J Glaucoma* 2006;15(1):40-46.

5 Chauhan BC, Danthurebandara VM, Sharpe GP, Demirel S, Girkin CA, Mardin CY, Scheuerle AF, Burgoyne CF. Bruch's membrane opening minimum rim width and retinal nerve fiber layer thickness in a normal white population: a multicenter study. *Ophthalmology* 2015; 122(9):1786-1794.

6 Schulze A, Lamparter J, Pfeiffer N, Berisha F, Schmidtmann I, Hoffmann EM. Diagnostic ability of retinal ganglion cell complex, retinal nerve fiber layer, and optic nerve head measurements by Fourier-domain optical coherence tomography. *Graefes Arch Clin Exp Ophthalmol* 2011;249(7):1039-1045.

7 Chauhan BC, O'Leary N, AlMobarak FA, Reis ASC, Yang HL, Sharpe GP, Hutchison DM, Nicolela MT, Burgoyne CF. Enhanced detection of open-angle glaucoma with an anatomically accurate optical coherence tomography-derived neuroretinal rim parameter. *Ophthalmology* 2013;120(3):535-543.

8 Sommer A, Katz J, Quigley HA, Miller NR, Robin AL, Richter RC, Witt KA. Clinically detectable nerve fiber atrophy precedes the onset of glaucomatous field loss. *Arch Ophthalmol* 1991;109(1):77-83.

9 Tan O, Chopra V, Lu ATH, Schuman JS, Ishikawa H, Wollstein G, Varma R, Huang D. Detection of macular ganglion cell loss in glaucoma by Fourier-domain optical coherence tomography. *Ophthalmology* 2009;116(12):2305-2314.e1-2.

10 Kim HJ, Lee SY, Park KH, Kim DM, Jeoung JW. Glaucoma diagnostic ability of layer-by-layer segmented ganglion cell complex by spectral-domain optical coherence tomography. *Invest Ophthalmol Vis Sci* 2016;57(11):4799-4805.

11 Elbendary AM, Abd El-Latef MH, Elsorogy HI, Enaam KM. Diagnostic accuracy of ganglion cell complex substructures in different stages of primary open-angle glaucoma. *Can J Ophthalmol* 2017;52(4):355-360.

12 Chien JL, Ghassibi MP, Patthanathamrongkasem T, Abumasmah R, Rosman MS, Skaat A, Tello C, Liebmann JM, Ritch R, Park SC. Glaucoma diagnostic capability of global and regional measurements of isolated ganglion cell layer and inner plexiform layer. *J Glaucoma* 2017;26(3):208-215.

13 Shin JW, Sung KR, Lee GC, Durbin MK, Cheng D. Ganglion cell-inner plexiform layer change detected by optical coherence tomography indicates progression in advanced glaucoma. *Ophthalmology* 2017;124(10):1466-1474.

14 Na JH, Sung KR, Baek SH, Kim ST, Shon K, Jung JJ. Rates and patterns of macular and circumpapillary retinal nerve fiber layer thinning in preperimetric and perimetric glaucomatous eyes. *J Glaucoma* 2015;24(4):278-285.

15 Akil H, Huang AS, Francis BA, Sadda SR, Chopra V. Retinal vessel density from optical coherence tomography angiography to differentiate early glaucoma, pre-perimetric glaucoma and normal eyes. *PLoS One* 2017;12(2):e0170476.

16 Kim YJ, Kang MH, Cho HY, Lim HW, Seong M. Comparative study of macular ganglion cell complex thickness measured by spectral-domain optical coherence tomography in healthy eyes, eyes with preperimetric glaucoma, and eyes with early glaucoma. *Jpn J Ophthalmol* 2014;58(3):244-251.

17 Kim HJ, Park KH, Kim YK, Jeoung JW. Evaluation of layer-by-layer segmented ganglion cell complex thickness for detecting early glaucoma according to different macular grids. *J Glaucoma* 2017; 26(8):712-717.

18 Danthurebandara VM, Sharpe GP, Hutchison DM, Denniss J, Nicolela MT, McKendrick AM, Turpin A, Chauhan BC. Enhanced structure-function relationship in glaucoma with an anatomically and geometrically accurate neuroretinal rim measurement. *Invest Ophthalmol Vis Sci* 2014;56(1):98-105.

19 Pollet-Villard F, Chiquet C, Romanet JP, Noel C, Aptel F. Structure-function relationships with spectral-domain optical coherence tomography retinal nerve fiber layer and optic nerve head measurements. *Invest Ophthalmol Vis Sci* 2014;55(5):2953-2962.

20 Gmeiner JMD, Schrems WA, Mardin CY, Laemmer R, Kruse FE, Schrems-Hoesl LM. Comparison of bruch's membrane opening minimum rim width and peripapillary retinal nerve fiber layer thickness in early glaucoma assessment. *Invest Ophthalmol Vis Sci* 2016;57(9):OCT575-OCT584.

21 Kromer R, Spitzer MS. Bruch's membrane opening minimum rim width measurement with SD-OCT: a method to correct for the opening size of Bruch's membrane. *J Ophthalmol* 2017;2017:8963267.

22 Bambo MP, Fuentemilla E, Cameo B, Fuertes I, Ferrandez B, Güerri N, Polo V, Larrosa JM, Pablo LE, Garcia-Martin E. Diagnostic capability of a linear discriminant function applied to a novel Spectralis OCT glaucoma-detection protocol. *BMC Ophthalmol* 2020;20(1):35.

23 Malik R, Belliveau AC, Sharpe GP, Shuba LM, Chauhan BC, Nicolela MT. Diagnostic accuracy of optical coherence tomography and scanning laser tomography for identifying glaucoma in myopic eyes. *Ophthalmology* 2016;123(6):1181-1189.

24 Chauhan BC, Vianna JR, Sharpe GP, Demirel S, Girkin CA, Mardin CY, Scheuerle AF, Burgoyne CF. Differential effects of aging in the macular retinal layers, neuroretinal rim, and peripapillary retinal nerve fiber layer. *Ophthalmology* 2020;127(2):177-185.

25 Curcio CA, Allen KA. Topography of ganglion cells in human retina. *J Comp Neurol* 1990;300(1):5-25.

26 Jeong JS, Kang MG, Kim CY, Kim NR. Pattern of macular ganglion cell-inner plexiform layer defect generated by spectral-domain OCT in glaucoma patients and normal subjects. *J Glaucoma* 2015;24(8):583-590.

27 Vidas S, Popović-Suić S, Novak Lauš K, Jandroković S, Tomić M, Jukić T, Kalauz M. Analysis of ganglion cell complex and retinal nerve fiber layer thickness in glaucoma diagnosis. *Acta Clin Croat* 2017;56(3):382-390.

28 Pillay G, Ganger A, Singh D, Bhatia R, Sharma P, Menon V, Saxena R. Retinal nerve fiber layer and ganglion cell layer changes on optical coherence tomography in early multiple sclerosis and optic neuritis cases. *Indian J Ophthalmol* 2018;66(1):114-119.

29 Rebolleda G, Diez-Alvarez L, Casado A, Sánchez-Sánchez C, de Dompablo E, González-López JJ, Muñoz-Negrete FJ. OCT: new perspectives in neuro-ophthalmology. *Saudi J Ophthalmol* 2015; 29(1):9-25.

30 Oddone F, Lucenteforte E, Michelessi M, Rizzo S, Donati S, Parravano M, Virgili G. Macular versus retinal nerve fiber layer parameters for diagnosing manifest glaucoma: a systematic review of diagnostic accuracy studies. *Ophthalmology* 2016;123(5):939-949.

31 Kansal V, Armstrong JJ, Pintwala R, Hutnik C. Optical coherence tomography for glaucoma diagnosis: an evidence based meta-analysis. *PLoS One* 2018;13(1):e0190621.

32 Deshpande G, Gupta R, Bawankule P, Raje D, Chakarborty M. Structural evaluation of preperimetric and perimetric glaucoma. *Indian J Ophthalmol* 2019;67(11):1843-1849.

33 Na JH, Lee K, Lee JR, Baek S, Yoo SJ, Kook MS. Detection of macular ganglion cell loss in preperimetric glaucoma patients with localized retinal nerve fibre defects by spectral-domain optical coherence tomography. *Clin Exp Ophthalmol* 2013;41(9):870-880.

34 Kaushik S, Kataria P, Jain V, Joshi G, Raj S, Pandav SS. Evaluation of macular ganglion cell analysis compared to retinal nerve fiber layer thickness for preperimetric glaucoma diagnosis. *Indian J Ophthalmol* 2018;66(4):511-516.

35 Xu XY, Xiao H, Guo XX, Chen XX, Hao LL, Luo JY, Liu X. Diagnostic ability of macular ganglion cell-inner plexiform layer thickness in glaucoma suspects. *Medicine* (*Baltimore*) 2017;96(51):e9182.